



This is a repository copy of *Highly efficient catalysis of the Kemp elimination in the cavity of a cubic coordination cage.*

White Rose Research Online URL for this paper:
<http://eprints.whiterose.ac.uk/95939/>

Version: Supplemental Material

Article:

Cullen, W., Misuraca, M.C., Hunter, C.A. et al. (2 more authors) (2016) Highly efficient catalysis of the Kemp elimination in the cavity of a cubic coordination cage. *Nature Chemistry*, 8 (3). pp. 231-236. ISSN 1755-4330

<https://doi.org/10.1038/nchem.2452>

Reuse

Unless indicated otherwise, fulltext items are protected by copyright with all rights reserved. The copyright exception in section 29 of the Copyright, Designs and Patents Act 1988 allows the making of a single copy solely for the purpose of non-commercial research or private study within the limits of fair dealing. The publisher or other rights-holder may allow further reproduction and re-use of this version - refer to the White Rose Research Online record for this item. Where records identify the publisher as the copyright holder, users can verify any specific terms of use on the publisher's website.

Takedown

If you consider content in White Rose Research Online to be in breach of UK law, please notify us by emailing eprints@whiterose.ac.uk including the URL of the record and the reason for the withdrawal request.



eprints@whiterose.ac.uk
<https://eprints.whiterose.ac.uk/>

Highly efficient catalysis of the Kemp elimination in the cavity of a cubic coordination cage

William Cullen, M. Cristina Misuraca, Christopher A. Hunter,* Nicholas H. Williams* and Michael D. Ward*

Supporting information

Experimental methods	p2
X-ray crystallography	p3
Figures S1 – S10	p6
Tables S1 – S3	p18

Experimental methods

General details

Instruments used for spectroscopic analyses were: (i) Cary 1-Bio for UV/Vis spectrophotometry; (ii) Bruker AV3-400 for ^1H NMR spectroscopy (both were thermostatted at 298K). The cage complex was prepared and purified as described previously.²³ All reagents were purchased from Sigma-Aldrich; the benzisoxazole is nominally '>95%' purity but NMR spectra, even at high concentrations, revealed no measurable impurities.

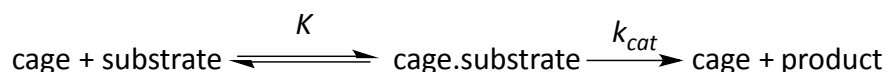
Monitoring the reaction.

Above pD 12, the uncatalysed Kemp elimination reaction was monitored by UV/Vis spectroscopy²⁹ at 298 K at various concentrations of NaOD (see Fig. S2) to obtain the black points in Fig. 2. The change in absorbance at 330 nm was fit to a first order rate equation to obtain the value for the observed rate constant k_{uncat} . At pD 10.2, the pD was controlled using a 0.1 M buffer solution containing $\text{NaHCO}_3 / \text{Na}_2\text{CO}_3$ to achieve the desired pD and the reaction monitored by ^1H NMR spectroscopy at 298 K.

The catalysed reaction, in the presence of the cage, could not be followed by UV/Vis spectroscopy due to the very strong absorptions of the cage in the UV/region which obscured the spectra of both the substrate benzisoxazole and product 2-cyanophenolate. Instead reactions were followed by ^1H NMR spectroscopy at 298 K, monitoring the intensity of product peaks close to 6.5 ppm which do not overlap with signals from either starting material or cage (Figs. S3 – S7, Table S1). The intensities of these were determined after local baseline correction and deconvolution of the signal from any nearby signals using the Bruker 'Topspin' software (see Fig. S8 for an example).

For the catalysis experiments the cage concentration was 1 mM in D_2O : in the absence of added base this solution is weakly acidic, and the pD was increased as required to a maximum of 11.4 by addition of portions of NaOD. The benzisoxazole starting material was then added to the NMR tube such that its concentration was 0.85 mM and ^1H NMR spectra were recorded at regular intervals. The pD was checked at the end of the reaction to ensure that it had not changed. To obtain k_{cat} , the appearance of product over time was fit to the Michaelis-Menten reaction scheme by numerical modeling with Berkeley MadonnaTM using the previously determined association constants for the substrate to the cage. Each measurement (at a particular pH) was repeated three times and an average taken.

Michaelis-Menten scheme used:



Since the product shows no evidence of binding to the cage nor of affecting the rate of the reaction of the substrate in the presence of the cage, and the expulsion of product from the cage cavity occurs on a sub-ms timescale (far faster than the rates of reaction), this simple Michaelis-Menten scheme can be used to model the catalysed reaction. At the pDs where the cage catalysed reactions were conducted, the background reaction was negligible (at least 100 fold slower than the catalysed reaction). K was described using a binding rate

constant of $10^6 \text{ M}^{-1} \text{ s}^{-1}$, and a dissociation rate constant of $2.5 \times 10^2 \text{ s}^{-1}$ to describe the measured binding constant of $4.0 \times 10^3 \text{ M}^{-1}$. The only variable in the numerical fitting procedure was k_{cat} .

Control experiments

(i) To determine the effect of a competitive inhibitor – and demonstrate that catalysis requires the guest to be bound in the cage cavity – the reaction in presence of catalyst was performed exactly as described above but with 20 mM cycloundecanone added; this binds in the cage much more strongly ($K = 1.2 \times 10^6 \text{ M}^{-1}$) than benzisoxazole.²⁶

(ii) To examine the effect of chloride ions, the catalysed reaction was monitored as described above but in the presence of 47 mM LiCl (higher concentrations than this resulted in decomposition of the cage). We note that the observed reaction is slightly slower than predicted for the background reaction alone, which can be explained by the substrate being protected from reaction when it binds to the cage surrounded by chloride ions.

(iii) To examine the effect of free Co(II) ions, the reaction was monitored as described above for the catalysed reactions but in the presence of 1 mM $\text{Co}(\text{BF}_4)_2$ instead of cage.

Data from all control experiments are shown in Fig. S9 and collected in Table S2.

Spontaneous reaction

The spontaneous reaction rate of benzisoxazole was estimated from the data in reference 27. The maximum rate constant for the spontaneous decomposition at 30 °C is reported as $1.1 \times 10^{-8} \text{ s}^{-1}$. Using the activation parameters for the hydroxide catalyzed reaction to estimate the reactivity at 25 °C leads to the estimate of $6 \times 10^{-9} \text{ s}^{-1}$ shown in fig. 3 in the main text (blue dotted line). This is a conservative estimate of the maximum observed rate constant for the spontaneous reaction.

X-ray crystallography

Crystallographic data for $[\text{Co}_8(\text{L}^{\text{W}})_{12}](\text{BF}_4)_{16} \cdot (\text{C}_7\text{H}_5\text{NO})$: $\text{C}_{360}\text{H}_{312}\text{B}_{16}\text{Co}_8\text{F}_{64}\text{N}_{73}\text{O}_{25}$, $M = 8010.32 \text{ g/mol}$, monoclinic, space group $C2/c$, $a = 27.2747(12)$, $b = 38.8257(17)$, $c = 42.232(2) \text{ \AA}$, $\beta = 108.089(3)^\circ$, $U = 42512(4) \text{ \AA}^3$, $Z = 4$, $\rho_{\text{calc}} = 1.252 \text{ g cm}^{-3}$, $T = 100(2) \text{ K}$, $\lambda(\text{Mo-K}\alpha) = 0.71073 \text{ \AA}$, $\mu = 0.402 \text{ mm}^{-1}$. 121554 reflections were merged to give 22378 independent reflections ($R_{\text{int}} = 0.15$). Final R_1 [for data with $I > 2\sigma(I)$] = 0.156; wR_2 (all data) = 0.452. The data collection was performed using a Bruker APEX-2 CCD diffractometer using Mo-K α radiation from a sealed-tube source. Data were corrected for absorption using empirical methods (SADABS) (ref. S1) based upon symmetry-equivalent reflections combined with measurements at different azimuthal angles. The structure was solved and refined using the SHELX suite of programs (ref. S2).

The asymmetric unit contains one half of the cage complex which lies astride an inversion centre, as well as one complete guest molecule whose atoms all have site occupancies of 0.5. Thus, the complete complex contains one guest molecule disordered over 2 symmetrically equivalent orientations with the N/O atoms pointing towards diagonally opposite corners Co(1) and Co(1A). The usual severe disorder of anions / solvent molecules and solvent loss characteristic of cage complexes of this type resulted in weak scattering, necessitating use of extensive geometric and displacement restraints to keep the

refinement stable: these are described in detail in the CIF. We could locate and refine six of the expected eight $[\text{BF}_4]^-$ anions in the asymmetric unit; all show disorder of the F atoms. Large regions of diffuse electron density which could not be modelled, accounting for the remaining anions plus solvent molecules, were eliminated from the refinement using of the 'SQUEEZE' function in the PLATON software package (ref. S3). The structural determination is therefore of poor quality by conventional small-molecule standards although it is typical for a coordination cage. The gross structure of the cage, and the presence of the guest in the cavity and its position / orientation in the cavity, are clear and we make no claims for structural details beyond this. CCDC deposition number: 1416694.

- S1 G. M. Sheldrick, SADABS: A program for absorption correction with the Siemens SMART system, University of Göttingen, Germany, 2008.
 S2 G. M. Sheldrick, *Acta Crystallogr. Sect. A*, 2008, **64**, 112.
 S3 A. Spek, *J. Appl. Cryst.*, 2003, **36**, 7; P. van der Sluis and A. L. Spek, *Acta Cryst. A*, 1990, **46**, 194.

The IUCR CheckCIF routine generates some category A and B alerts which are all related to the above-mentioned issues. Specifically:

Category A alerts:

(i) The three alerts below all relate to the weakness of the data

RFACR01_ALERT_3_A The value of the weighted R factor is > 0.45
 Weighted R factor given 0.454
 THETM01_ALERT_3_A The value of sine(theta_max)/wavelength is less than 0.550
 Calculated sin(theta_max)/wavelength = 0.5021
 PLAT026_ALERT_3_A Ratio Observed / Unique Reflections too Low 29 %

(ii) The five alerts below all relate to close OH•••HO distances between the periphery of adjacent cages in which the OH groups exhibit disorder

PLAT415_ALERT_2_A Short Inter D-H..H-X H17O .. H18F .. 1.87 Ang.
 PLAT415_ALERT_2_A Short Inter D-H..H-X H18B .. H33B .. 1.77 Ang.
 PLAT417_ALERT_2_A Short Inter D-H..H-D H18A .. H18C .. 1.68 Ang.
 PLAT417_ALERT_2_A Short Inter D-H..H-D H18D .. H18D .. 1.37 Ang.
 PLAT417_ALERT_2_A Short Inter D-H..H-D H38C .. H38C .. 1.72 Ang.

(iii) The alerts below relates to the diffuse electron density, corresponding to around 1000 electrons per complete complex, that was eliminated from the refinement using 'SQUEEZE'. This will comprise the fluoroborate anions that could not be located as well as solvent molecules from the crystallization (MeOH and water).

PLAT602_ALERT_2_A VERY LARGE Solvent Accessible VOID(S) in Structure ! Info

Category B alerts:

(i) The four alerts below are all normal for structures of this type and arise from the weakness of the scattering

RFACG01_ALERT_3_B The value of the R factor is > 0.15: R factor given 0.156
 PLAT082_ALERT_2_B High R1 Value 0.16 Report
 PLAT084_ALERT_3_B High wR2 Value (i.e. > 0.25) 0.45 Report
 PLAT341_ALERT_3_B Low Bond Precision on C-C Bonds 0.0156 Ang.

(ii) This alert arises from the missing $[\text{BF}_4]^-$ anions that could not be crystallographically located due to disorder but which were included in the formula

PLAT043_ALERT_1_B Calculated and Reported Mol. Weight Differ by .. 347.20 Check

(iii) The alerts below commonly arises around the heaviest atoms (here, Co) due to imperfect absorption correction arising from weak data

PLAT232_ALERT_2_B Hirshfeld Test Diff (M-X) Co3 -- N22A .. 11.2 su

PLAT232_ALERT_2_B Hirshfeld Test Diff (M-X) Co3 -- N31D .. 13.8 su

(iv) The alerts below arise because the peripheral OH groups do not have clearly identified H-bond acceptors and likely arises due to the fact that disordered solvent molecules were removed using SQUEEZE.

PLAT420_ALERT_2_B D-H Without Acceptor O18B - H18B .. Please Check

PLAT420_ALERT_2_B D-H Without Acceptor O18E - H18E .. Please Check

PLAT420_ALERT_2_B D-H Without Acceptor O18F - H18F .. Please Check

PLAT420_ALERT_2_B D-H Without Acceptor O18H - H18H .. Please Check

PLAT420_ALERT_2_B D-H Without Acceptor O38A - H38A .. Please Check

PLAT420_ALERT_2_B D-H Without Acceptor O38B - H38B .. Please Check

PLAT420_ALERT_2_B D-H Without Acceptor O38D - H38D .. Please Check

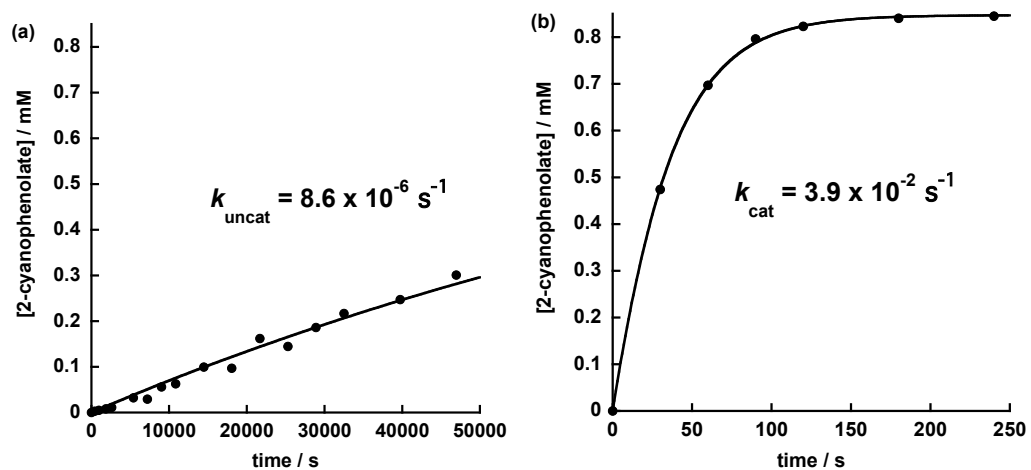


Fig. S1 Comparison of rates of (a) uncatyzed and (b) catalyzed reactions based on the conditions described in the caption to Fig. 3, at pD 10.2: $k_{\text{cat}}/k_{\text{uncat}} = 4500$.

Fig. S2: Kinetic data for the background reaction (no catalyst present). Appearance of 2-cyanophenolate was measured by its absorbance at 330 nm. This data was used to plot the black line in Fig. 2 of the main text.

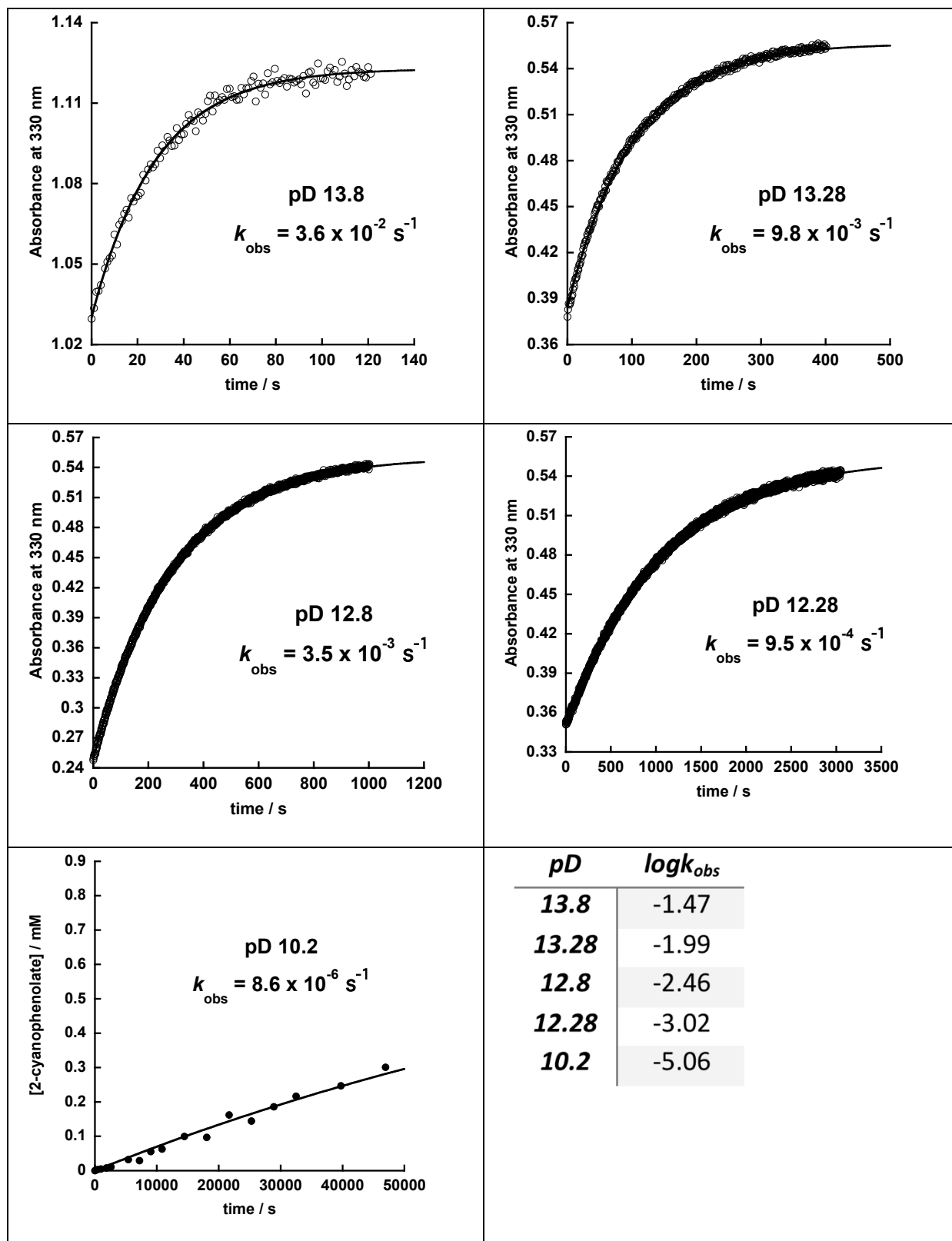
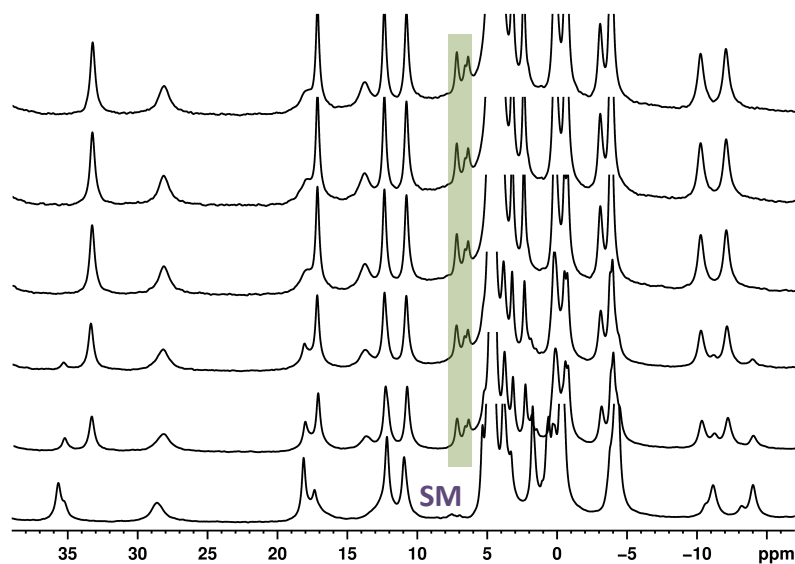
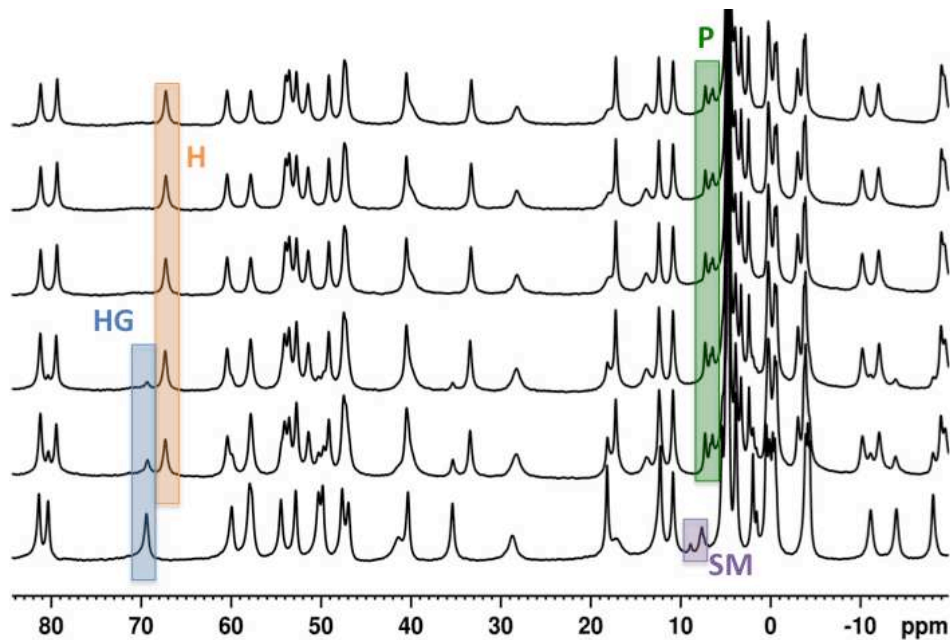


Fig. S3: Kinetic Data - Catalysed reaction at pD 8.5. Top: evolution of NMR spectra [SM = starting material (benzoxazole); P = product (2-cyanophenolate); HG = host/guest complex with bound benzoxazole; H = empty host cage] with expansion underneath showing the grow-in of product peaks, highlighted in green. Overleaf: kinetic traces of product evolution from three independent experiments.



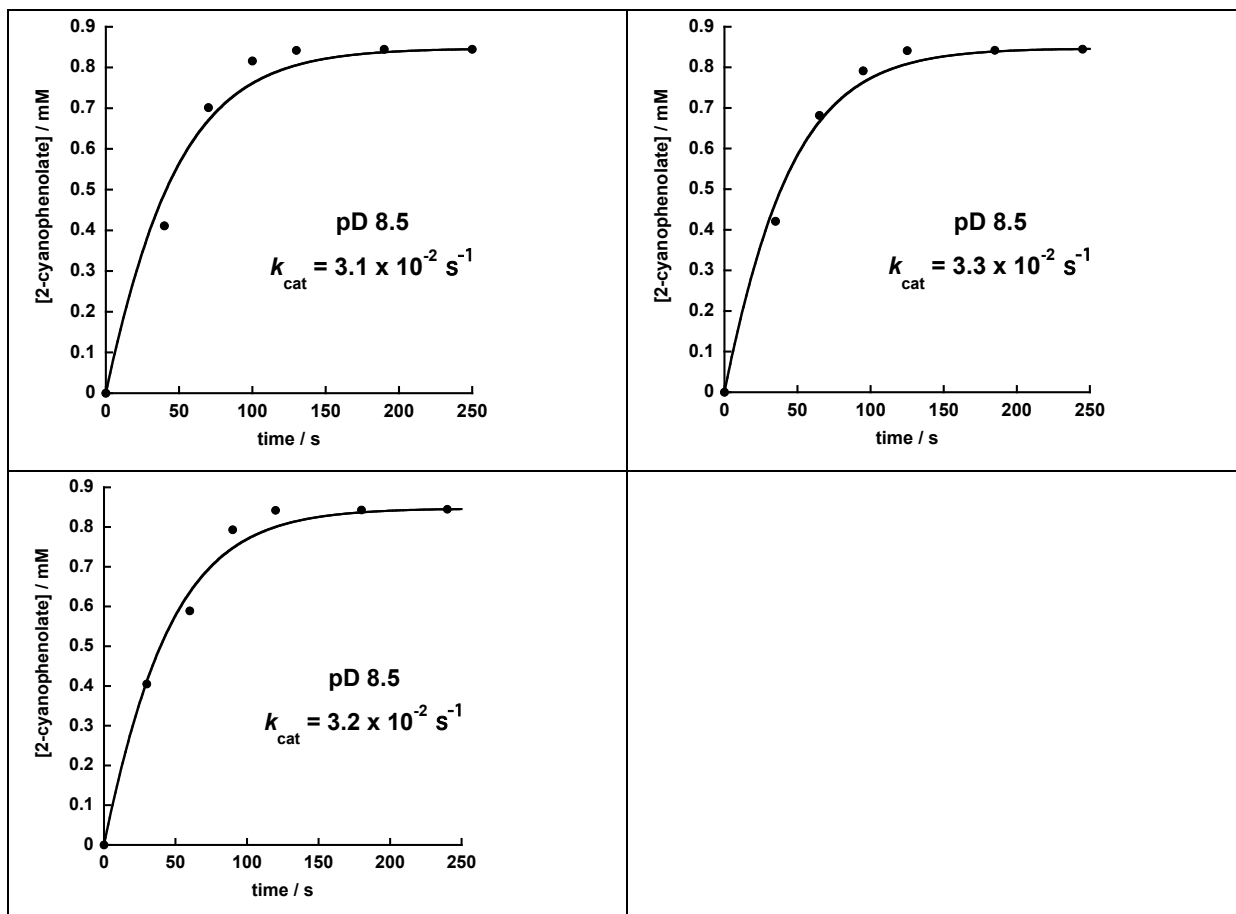


Fig. S4: Kinetic Data - Catalysed reaction at pD 9.4. Top: evolution of NMR spectra [SM = starting material (benzoxazole); P = product (2-cyanophenolate); HG = host/guest complex with bound benzoxazole; H = empty host cage]. Bottom: kinetic traces of product evolution from three independent experiments.

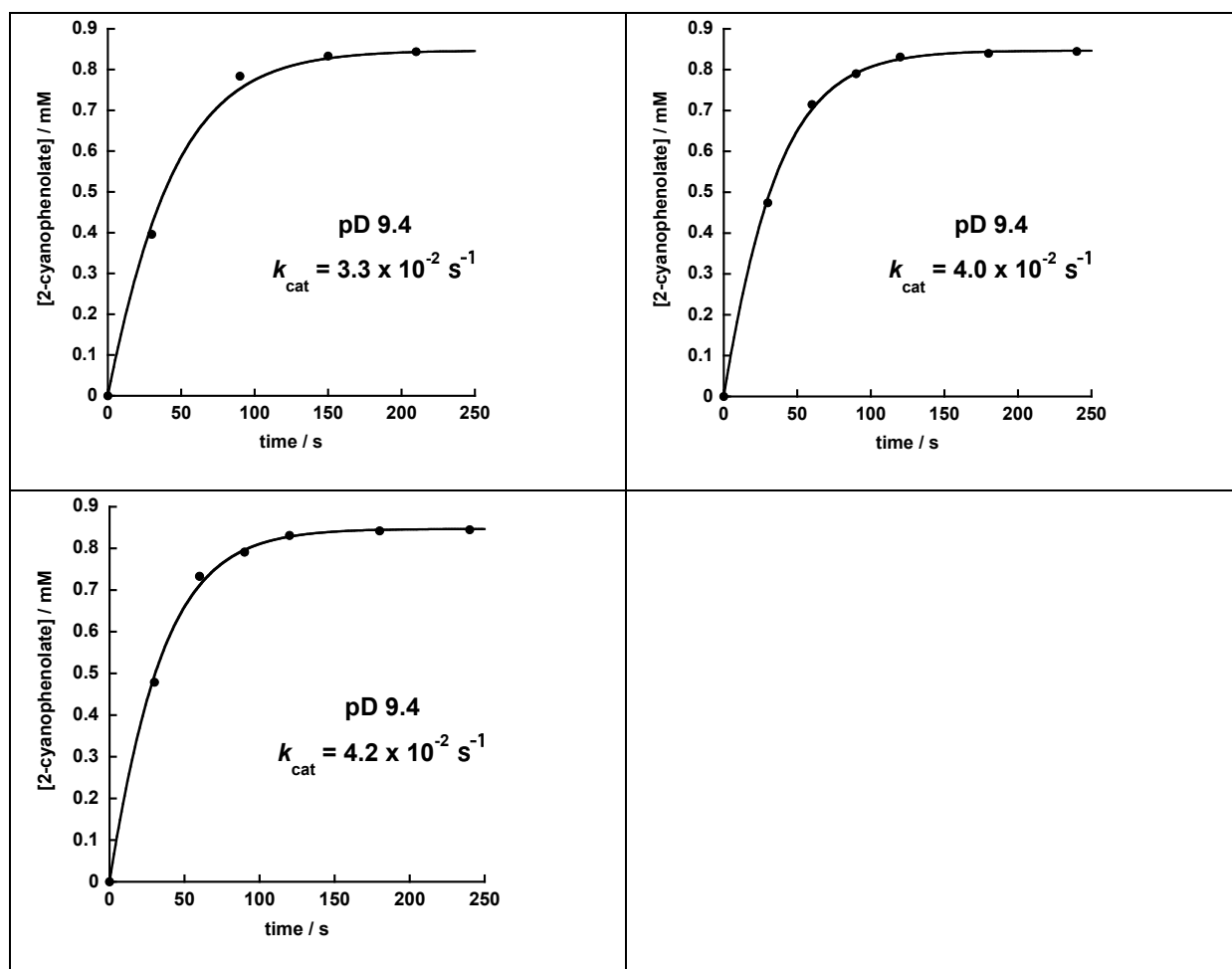
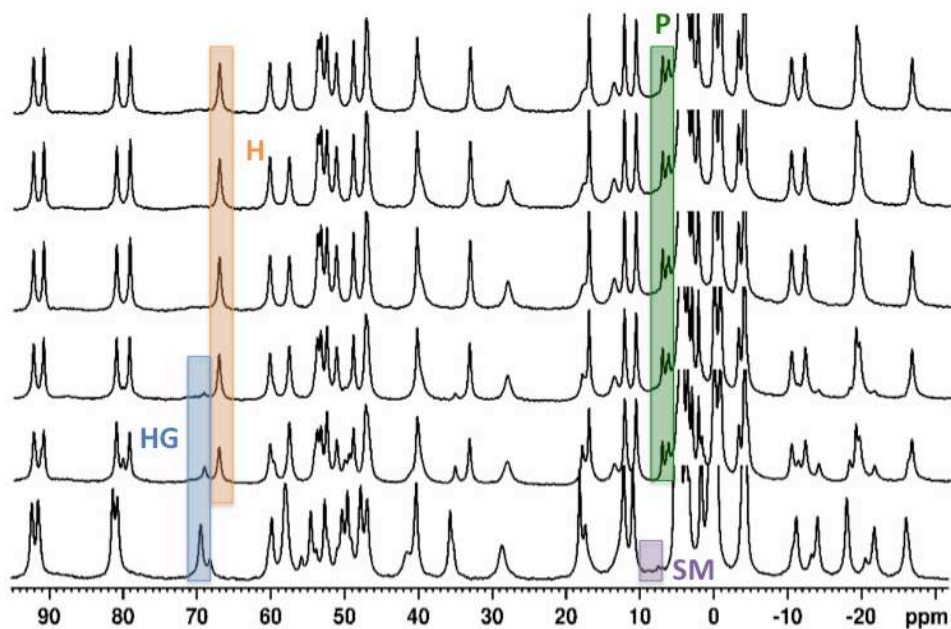


Fig. S5: Kinetic Data - Catalysed reaction at pD 10.2. Top: evolution of NMR spectra [SM = starting material (benzisoazole); P = product (2-cyanophenolate); HG = host/guest complex with bound benzisoazole; H = empty host cage]. Bottom: kinetic traces of product evolution from three independent experiments.

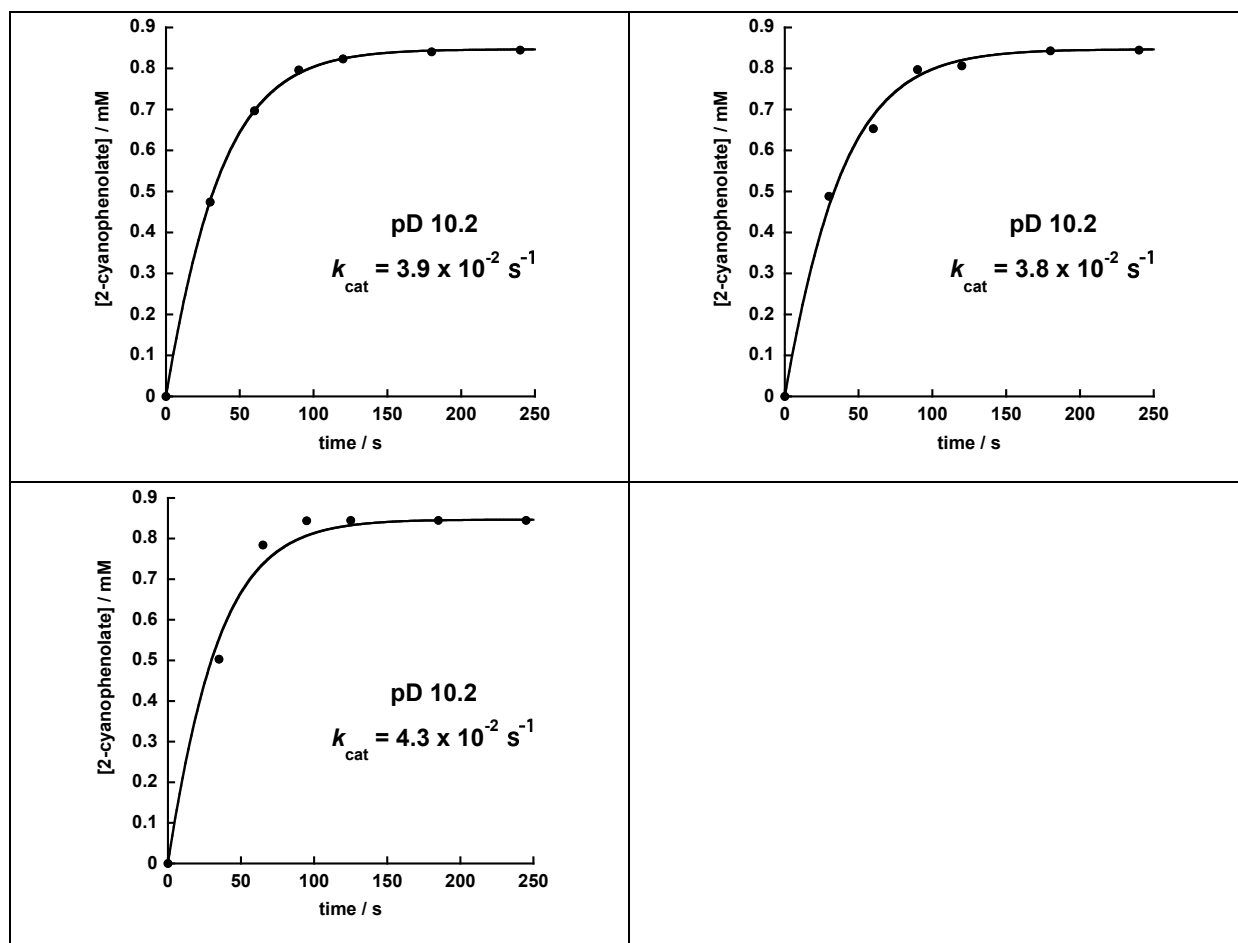
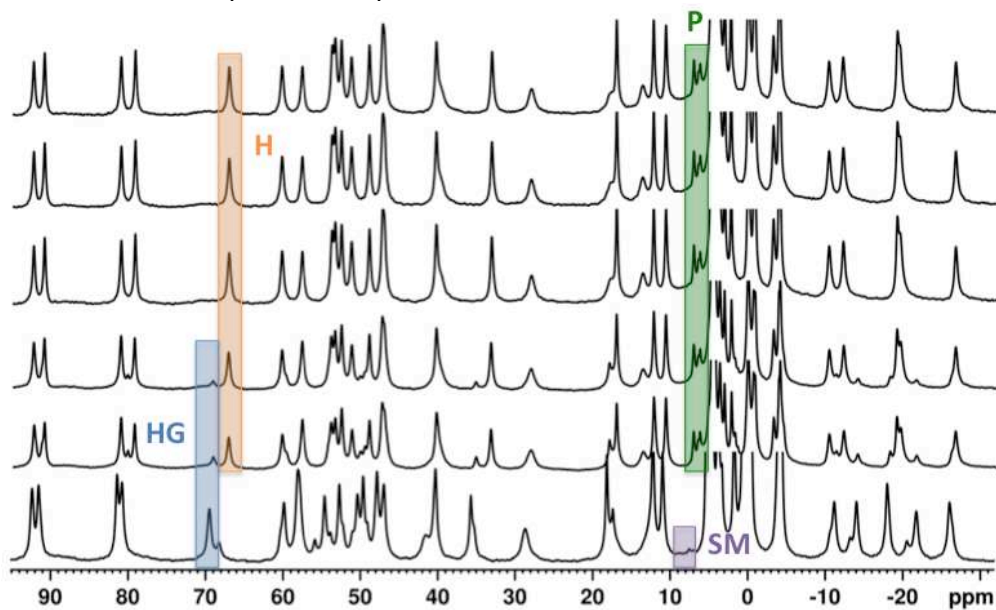


Fig. S6: Kinetic Data - Catalysed reaction at pD 10.7. Top: evolution of NMR spectra [SM = starting material (benzoxazole); P = product (2-cyanophenolate); HG = host/guest complex with bound benzoxazole; H = empty host cage]. Bottom: kinetic traces of product evolution from three independent experiments.

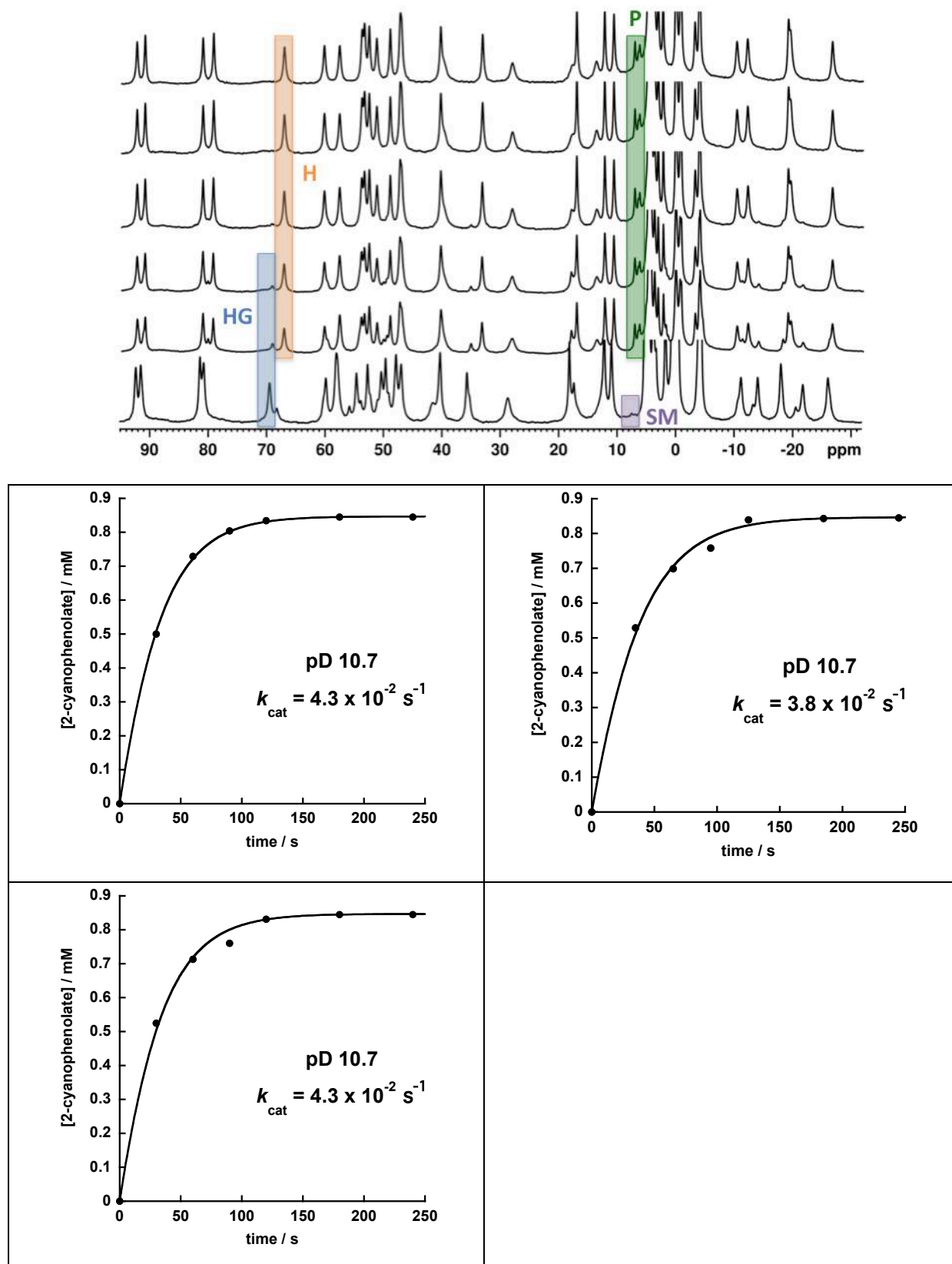


Fig. S7: Kinetic Data - Catalysed reaction at pD 11.3. Top: evolution of NMR spectra [SM = starting material (benzisoazole); P = product (2-cyanophenolate); HG = host/guest complex with bound benzisoazole; H = empty host cage]. Bottom: kinetic traces of product evolution from three independent experiments.

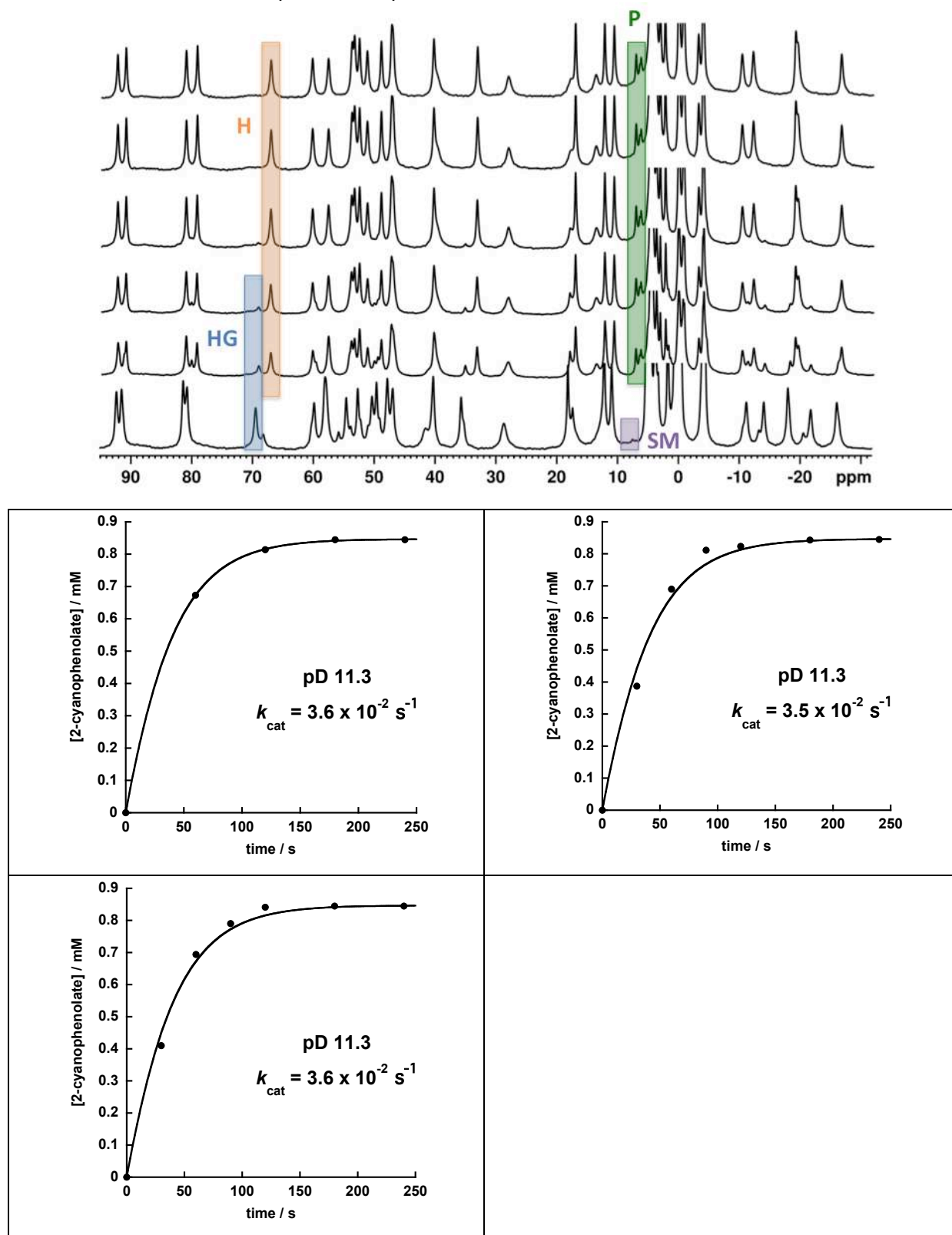


Fig. S8. Example of baseline-corrected / deconvoluted ^1H NMR signals of the product appearing at 6 – 8 ppm: integration of this signal formed the basis of the kinetic measurements.

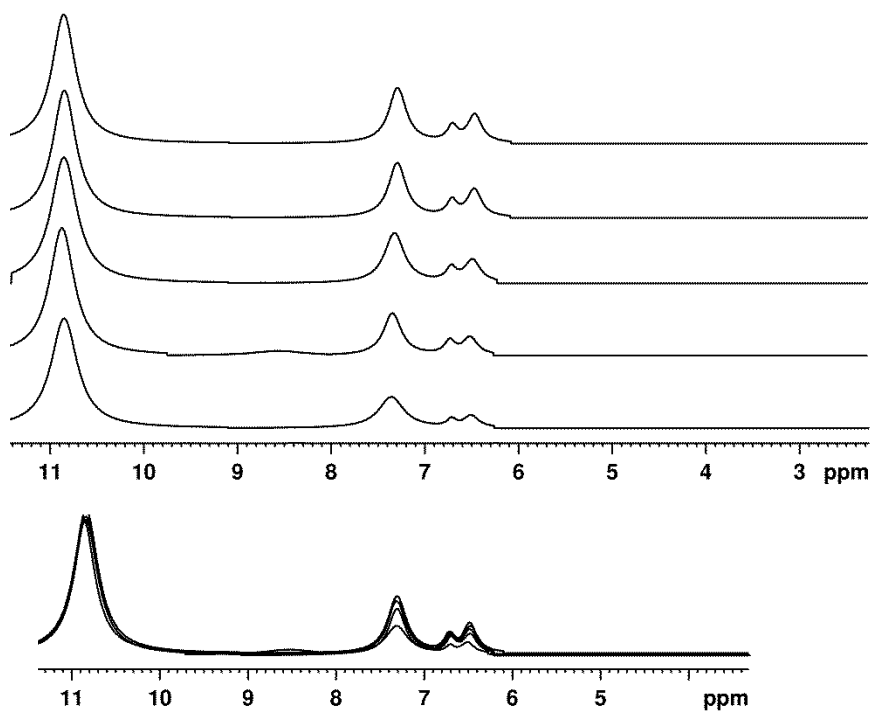
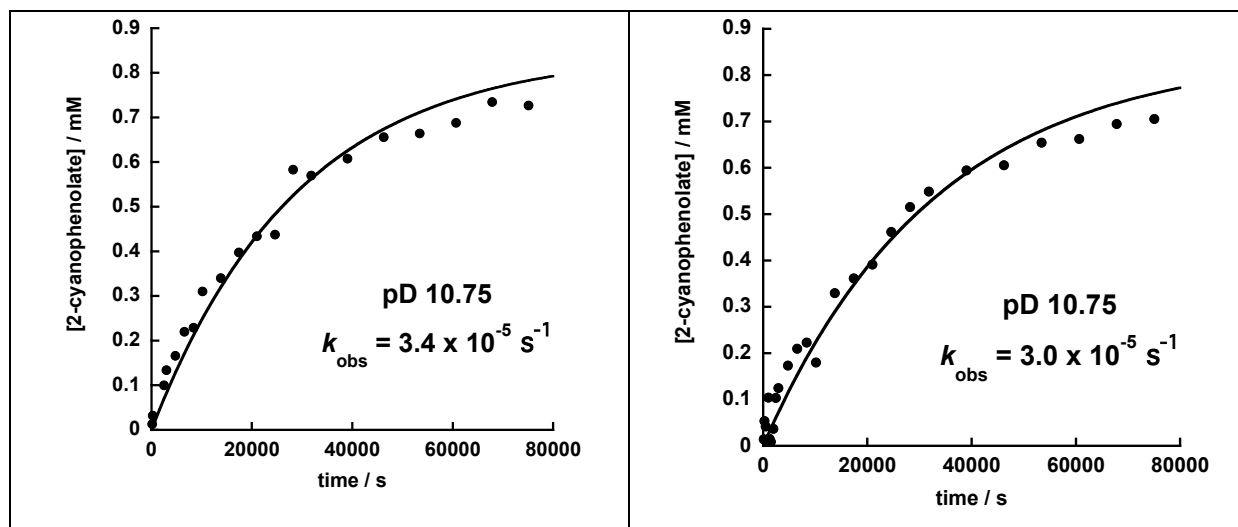
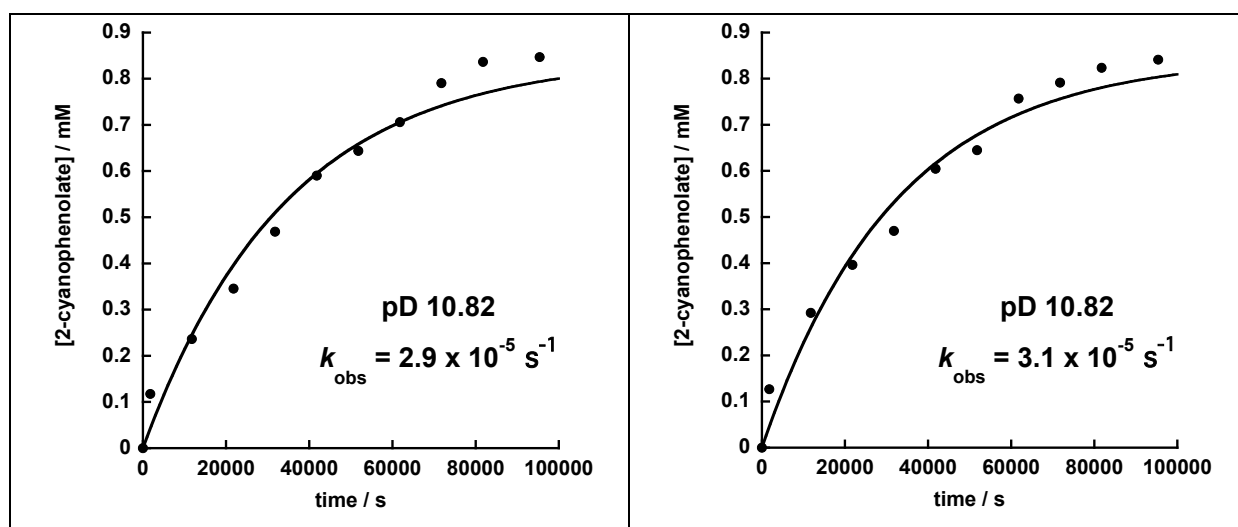


Fig. S9: Control experiments (as in Figs. S3 – S7, concentration of product is determined from integration of the NMR signals for 2-cyanophenolate at 6 – 7 ppm).

(i) Duplicate kinetic traces for reaction in presence of 20 mM cycloundecanone



(ii) Duplicate kinetic traces for reaction in presence of 47 mM LiCl



(iii) Top: evolution of NMR spectra for reaction in presence of 1 mM $\text{Co}(\text{BF}_4)_2$ but no catalyst (SM = starting material signals; P = product signals). Bottom: kinetic trace derived from this NMR data

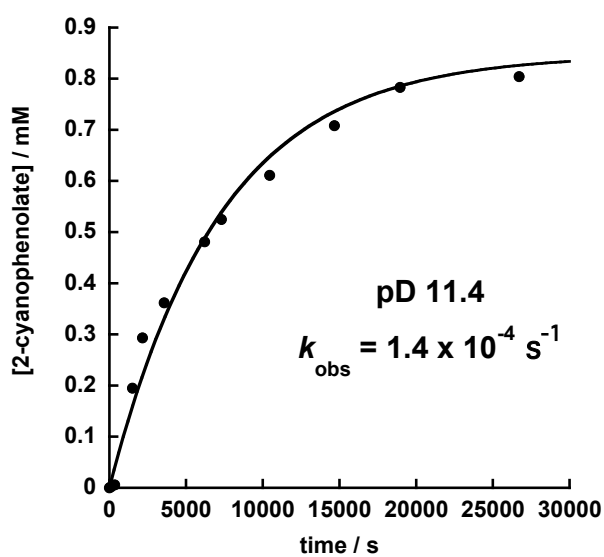
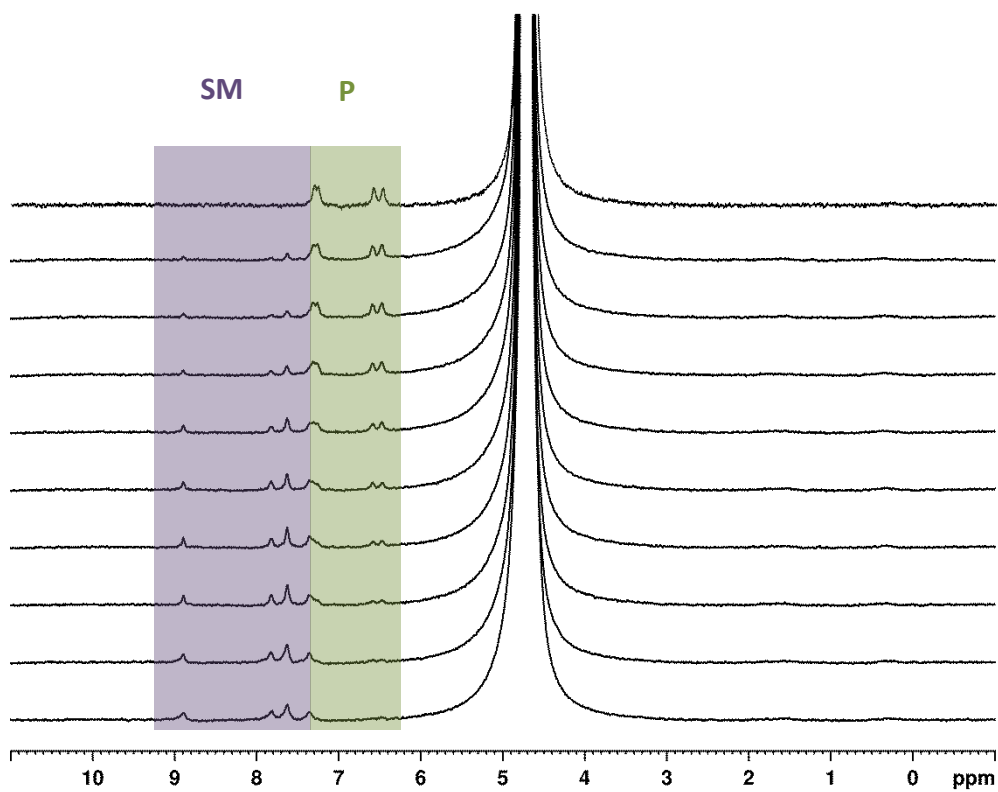


Fig. S10: Comparison of NMR spectra of free cage (bottom) and cage after catalysing 100 turnovers of the Kemp elimination reaction (top)

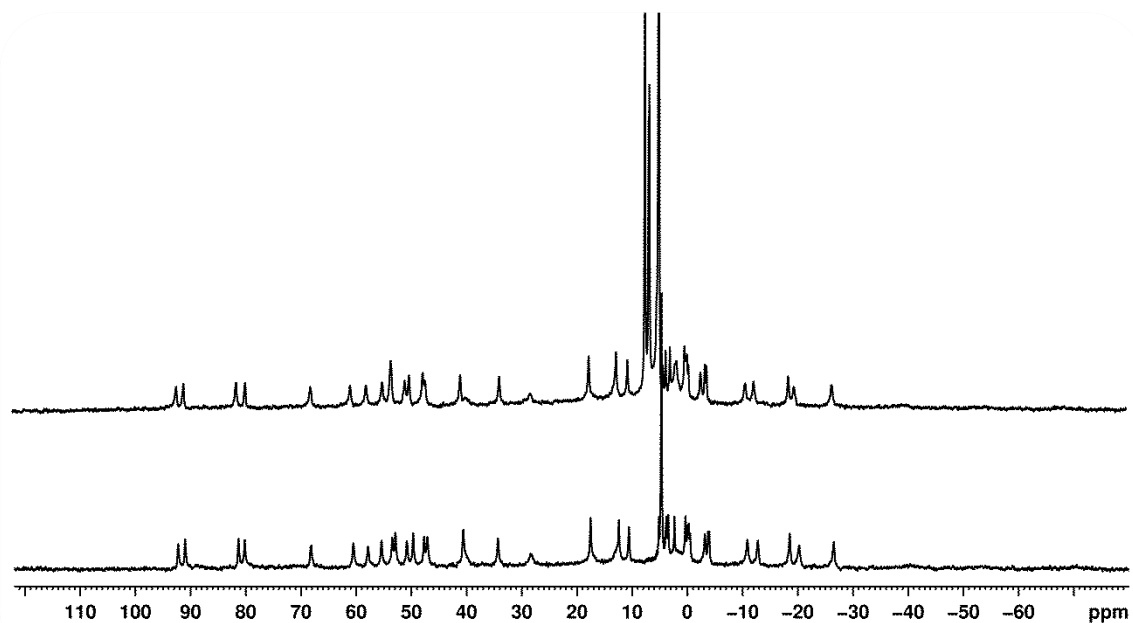


Table S1. Tabulated data for cage-catalyzed reactions (extracted from NMR spectra in Fig. S3 – S7) used in Fig. 3

pD 8.5		pD 9.4		pD 10.2		pD 10.7		pD 11.3	
t (s)	[Product] (M)	t (s)	[Product] (M)	t (s)	[Product] (M)	t (s)	[Product] (M)	t (s)	[Product] (M)
0	0.00E+00	0	0.00E+00	0	0.00E+00	0	0.00E+00	0	0.00E+00
40	4.11E-04	30	3.96E-04	30	4.74E-04	30	5.00E-04	60	6.73E-04
70	7.02E-04	90	7.84E-04	60	6.97E-04	60	7.29E-04	120	8.14E-04
100	8.16E-04	150	8.33E-04	90	7.96E-04	90	8.04E-04	180	8.45E-04
130	8.42E-04	210	8.44E-04	120	8.23E-04	120	8.34E-04	240	8.45E-04
190	8.45E-04	270	8.44E-04	180	8.41E-04	180	8.45E-04		
250	8.45E-04	330	8.47E-04	240	8.45E-04	240	8.45E-04		
		390	8.47E-04						
0	0.00E+00	0	0.00E+00	0	0.00E+00	0	0.00E+00	0	0.00E+00
35	4.21E-04	30	4.74E-04	30	4.88E-04	35	5.29E-04		3.87E-04
65	6.82E-04	60	7.15E-04	60	6.53E-04	65	6.99E-04	60	6.90E-04
95	7.91E-04	90	7.90E-04	90	7.97E-04	95	7.58E-04	90	8.11E-04
125	8.41E-04	120	8.31E-04	120	8.06E-04	125	8.39E-04	120	8.23E-04
185	8.42E-04	180	8.40E-04	180	8.43E-04	185	8.43E-04	180	8.43E-04
245	8.45E-04	240	8.45E-04	240	8.45E-04	245	8.45E-04	240	8.45E-04
0	0.00E+00	0	0.00E+00	0	0.00E+00	0	0.00E+00	0	0.00E+00
30	4.05E-04	30	4.79E-04	35	5.03E-04	30	5.25E-04	30	4.10E-04
60	5.89E-04	60	7.33E-04	65	7.84E-04	60	7.13E-04	60	6.94E-04
90	7.93E-04	90	7.91E-04	95	8.44E-04	90	7.60E-04	90	7.90E-04
120	8.42E-04	120	8.31E-04	125	8.45E-04	120	8.31E-04	120	8.41E-04
180	8.43E-04	180	8.42E-04	185	8.45E-04	180	8.45E-04	180	8.45E-04
240	8.45E-04	240	8.45E-04	245	8.45E-04	240	8.45E-04	240	8.45E-04

pD	k_{av}	Error(2 σ)	Log k_{av}
8.5	3.18E-02	2.00E-3	-1.497
9.4	3.82E-02	9.43E-3	-1.417
10.2	3.99E-02	5.29E-3	-1.399
10.7	4.12E-02	5.30E-3	-1.386
11.3	3.59E-02	1.15E-3	-1.445

The values for k_{av} (column 1) are based on the average of the three independent catalysis runs at each pD value; the quoted experimental uncertainty is twice the standard deviation generated by the curve-fitting analysis. The log k_{av} values (column 3) are those in Fig. 3 of the main text (red line); the uncertainties in the log k values are comparable to the height of the red dots used in Fig. 3.

Table S2. Tabulated data for control experiments based on NMR integrals for appearance of product

cycloundecanone				Cl-		Co(II) ions	
t / s	[Product] / M	t / s	[Product] / M	t / s	[Product] / M	t / s	[Product] / M
126	1.44E-05	156	1.31E-05	0	0.00E+00	0	0.00E+00
252	5.35E-05	282	3.20E-05	1800	1.18E-04	120	2.42E-06
378	1.29E-05	2490	1.00E-04	11800	2.36E-04	350	5.97E-06
504	4.19E-05	2976	1.34E-04	21800	3.46E-04	1500	1.95E-04
750	1.32E-05	4782	1.66E-04	31800	4.69E-04	2170	2.93E-04
996	1.04E-04	6588	2.20E-04	41800	5.90E-04	3580	3.62E-04
1242	1.53E-05	8394	2.29E-04	51800	6.44E-04	6210	4.81E-04
1488	8.83E-06	10200	3.10E-04	61800	7.06E-04	7311	5.25E-04
1974	3.67E-05	13806	3.40E-04	71800	7.90E-04	10450	6.11E-04
2460	1.03E-04	17412	3.98E-04	81800	8.36E-04	14670	7.08E-04
2946	1.25E-04	21018	4.34E-04	95400	8.47E-04	18960	7.83E-04
4752	1.73E-04	24624	4.37E-04			26710	8.04E-04
6558	2.10E-04	28230	5.83E-04				
8364	2.23E-04	31836	5.70E-04	0	0.00E+00		
10170	1.80E-04	39042	6.08E-04	1800	1.27E-04		
13776	3.30E-04	46248	6.56E-04	11800	2.92E-04		
17382	3.61E-04	53454	6.64E-04	21800	3.96E-04		
20988	3.91E-04	60660	6.88E-04	31800	4.70E-04		
24594	4.61E-04	67866	7.35E-04	41800	6.05E-04		
28200	5.15E-04	75072	7.27E-04	51800	6.45E-04		
31806	5.49E-04			61800	7.57E-04		
39012	5.95E-04			71800	7.92E-04		
46218	6.06E-04			81800	8.24E-04		
53424	6.54E-04			95400	8.41E-04		
60630	6.62E-04						
67836	6.95E-04						
75042	7.06E-04						

Control type	pD	$k_{av} (s^{-1})$	Error(2 σ)	log k_{av}
cycloundecanone	10.75	3.07E-05	5.66E-6	-4.513
Cl-	10.82	2.90E-05	2.83E-6	-4.538
Co(II) ions	11.4	1.39E-04		-3.858

As with the catalysed reactions, the error in the log k values are comparable to the height of the circles used to depict the data points in Fig. 3.

Table S3. Tabulated Data for turnover experiment (see Fig. 6). Accumulation of 2-cyanophenolate following addition of a series of aliquots of benzisoxazole substrate (0.85 equivalents each) to a solution of cage (1 mM) in D₂O at pD 10.2. Aliquots of substrate were added at 720 second intervals, giving a total of 4.2 turnovers for this set of data.

T / s	[Cumulative product]		
0	0.00E+00	2160	2.54E-03
30	4.74E-04	2160	2.54E-03
90	6.97E-04	2190	3.00E-03
180	7.96E-04	2250	3.24E-03
300	8.23E-04	2340	3.34E-03
480	8.41E-04	2460	3.38E-03
720	8.45E-04	2640	3.38E-03
720	8.45E-04	2880	3.38E-03
750	1.34E-03	2880	3.38E-03
810	1.57E-03	2910	3.84E-03
900	1.65E-03	2970	4.08E-03
1020	1.66E-03	3060	4.18E-03
1200	1.68E-03	3180	4.22E-03
1440	1.69E-03	3360	4.23E-03
1440	1.69E-03	3600	4.23E-03
1470	2.16E-03		
1530	2.37E-03		
1620	2.48E-03		
1740	2.52E-03		
1920	2.54E-03		